Supplementary Material (ESI) for Dalton Transactions

Photoreactive Ru(II)-oligonucleotide conjugates: influence of an intercalating ligand on the inter- and intra-strand photo-ligation processes

Stéphane Le Gac, Martin Foucart, Pascal Gerbaux, Eric Defrancq, Cécile Moucheron, Andrée Kirsch - De Mesmaeker

Supporting Information

Contents:

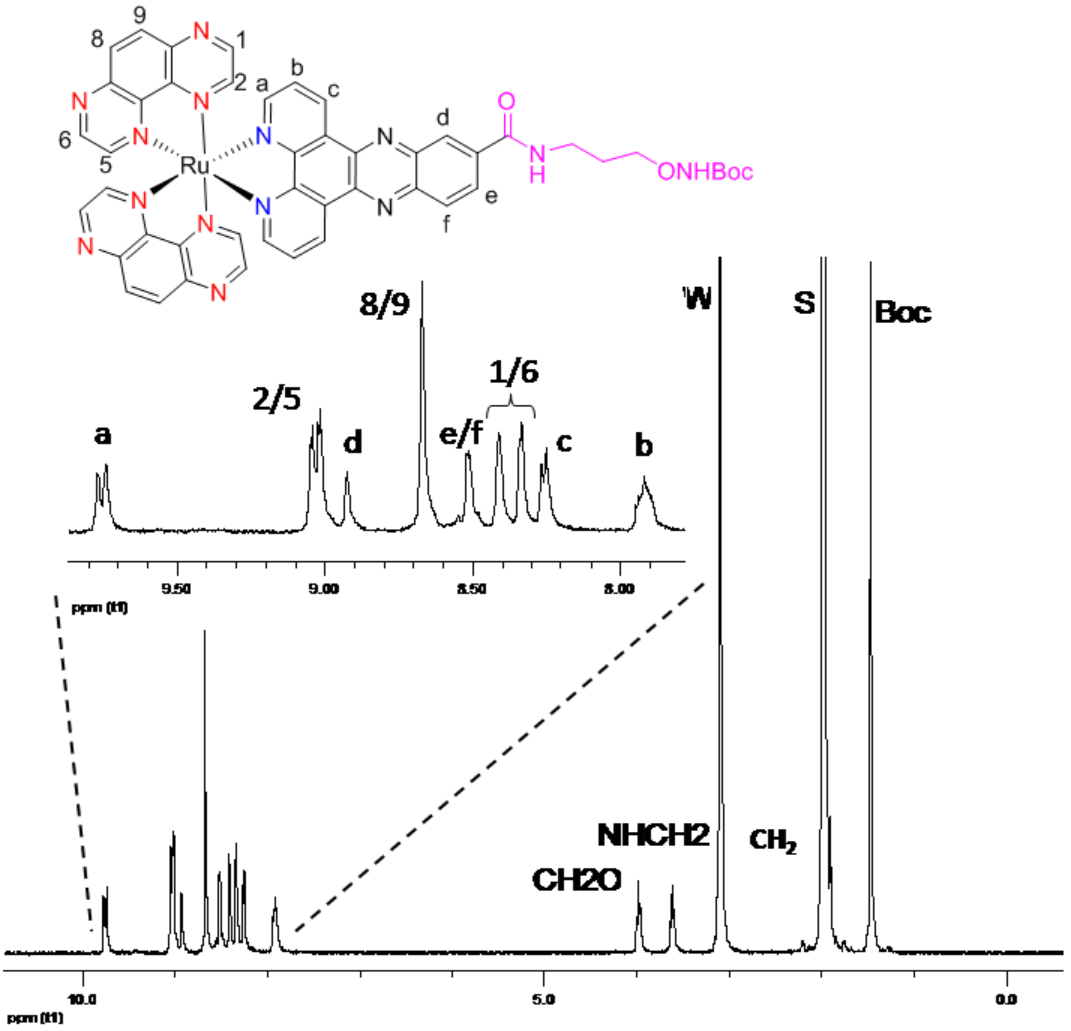

Figure S1. ^{1}H NMR spectrum (CD_3CN/D_2O 10:1) of the **[Ru(TAP)$_2$(dppz")]$^{2+}$** complex (W = water, S = solvent).

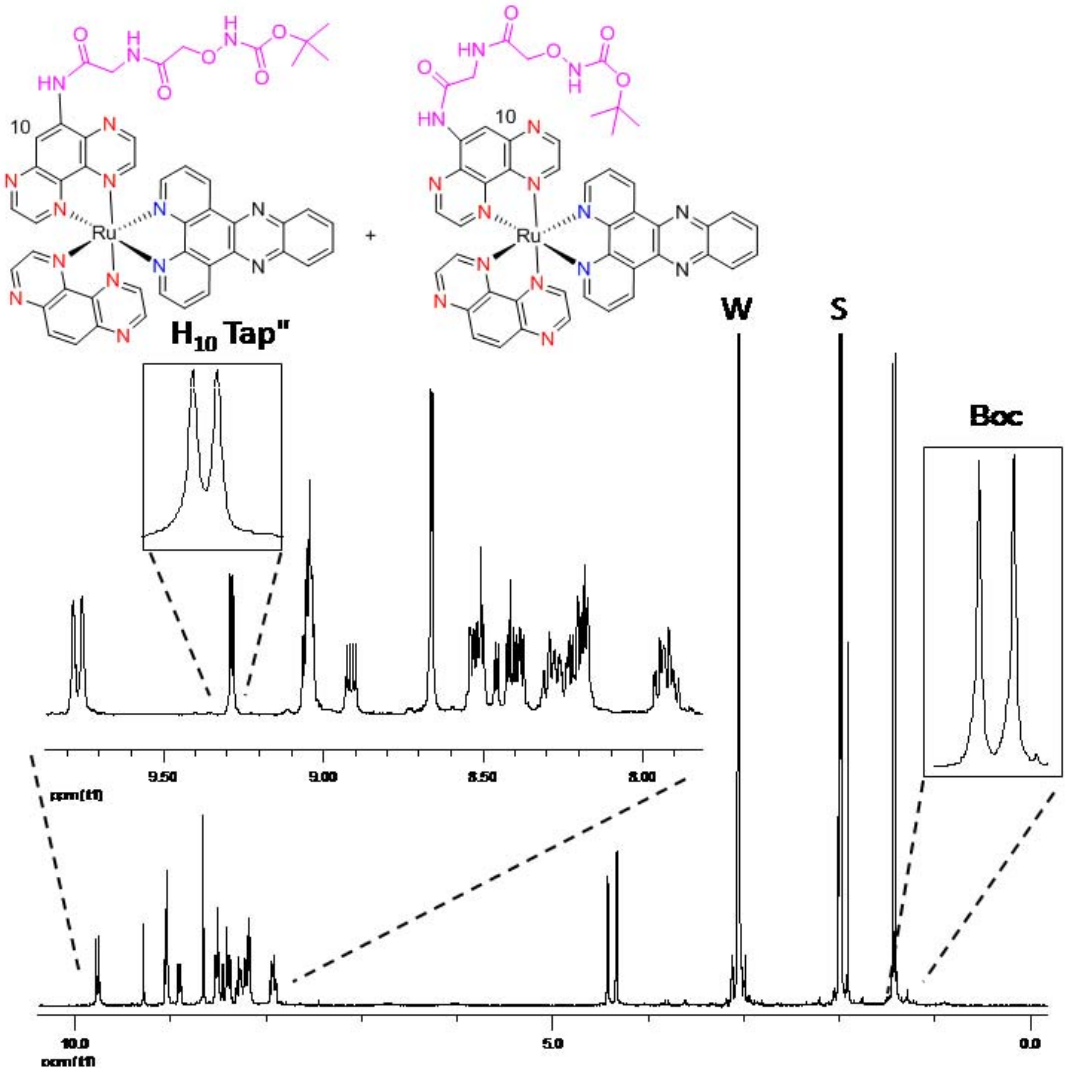

Figure S2. ^{1}H NMR spectrum (CD_3CN/D_2O 10:1) of the **[Ru(TAP)(dppz)(TAP")]$^{2+}$** complex (1:1 mixture of two isomers) (W = water, S = solvent).

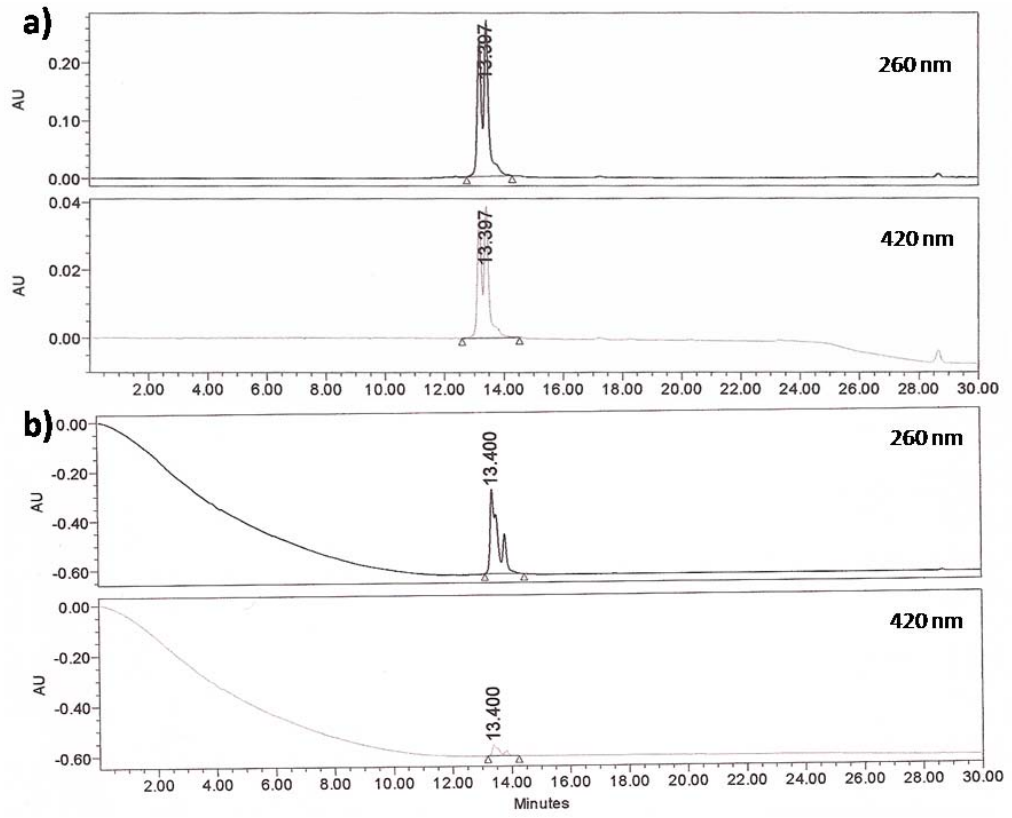

Figure S3. HPLC chromatograms (reverse phase) of Ru-ODN conjugates **Ru(D)-ODN$_{(G)}$** (a) and **Ru(T)-ODN$_{(G)}$** (b) after PAGE purification.

Additional comments: the HPLC trace of **Ru(D)-ODN$_{(G)}$** shows two peaks in a 1:1 ratio, either with a detection at 260 nm (ODN absorbance) or 420 nm (Ru^{II} complex absorbance). In the case of **Ru(T)-ODN$_{(G)}$**, the HPLC trace is more complicated with overlapping of several peaks, but with the same profile at the two wavelengths. This is likely due to the cis-trans isomerism of the oxime bond that leads to two diastereomeric ODN-conjugates in the case of **Ru(D)-ODN$_{(G)}$**. The situation is more complicated with **Ru(T)-ODN$_{(G)}$** since the **[Ru(TAP)(dppz)(TAP")]$^{2+}$** complex is present as two geometrical isomers. Thus, four isomers are possible from the bioconjugation. Because of the partial overlapping of the HPLC signals, the different isomers could not be separated by preparative HPLC. PAGE analyses of the samples of **Ru(D)-ODN$_{(G)}$** and **Ru(T)-ODN$_{(G)}$** revealed only one band.

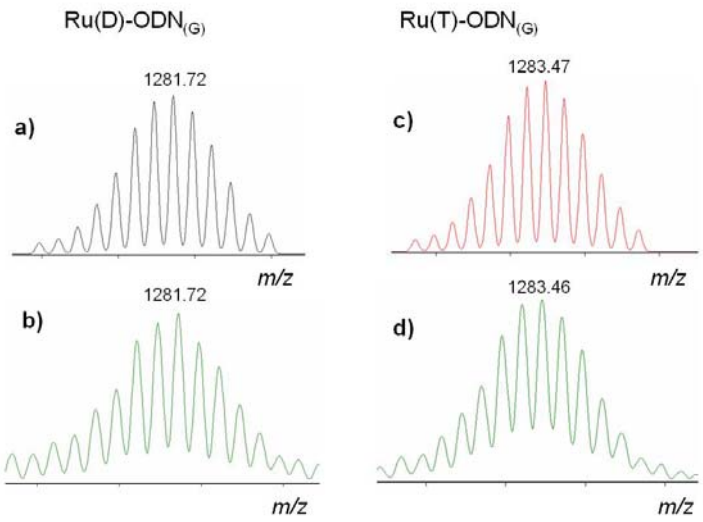

Figure S4. Nano-ESI mass spectra (positive ion mode), comparison between the experimental data and isotopic pattern simulations (IPS) for **Ru(D)-ODN$_{(G)}$** and **Ru(T)-ODN$_{(G)}$** (expanded views for the isotopic distributions): a) IPS for a four-fold charged cation corresponding to **Ru(D)-ODN$_{(G)}$** ($C_{177}H_{204}N_{58}O_{89}P_{14}Ru + H^+ + Na^+$); b) experimental mass spectrum obtained for **Ru(D)-ODN$_{(G)}$**; c) IPS for a four-fold charged cation corresponding to **Ru(T)-ODN$_{(G)}$** ($C_{177}H_{203}N_{59}O_{90}P_{14}Ru + 2H^+$); d) experimental mass spectrum obtained for **Ru(T)-ODN$_{(G)}$**.

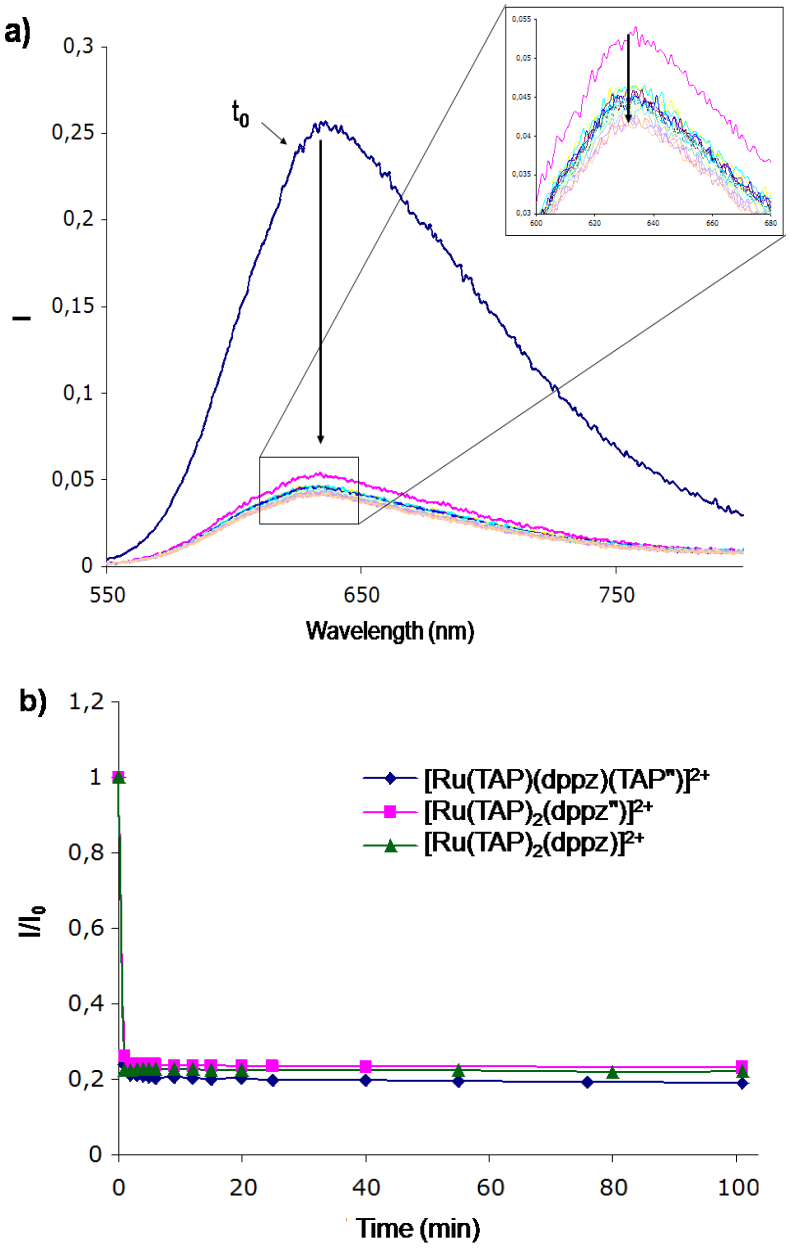

Figure S5. (a) Time evolution of the emission spectrum of the free **Ru(T)** complex after addition of CT-DNA (up to 100 min); conditions: [**Ru(T)**] = 5 µM, P/Ru = 100, [NaCl] = 150 mM, TrisHCl = 10 mM (pH 7). (b) Kinetic trace related to the interaction of the free **[Ru(TAP)$_2$(dppz)]$^{2+}$** complex and derivatives **Ru(D)** and **Ru(T)** with CT-DNA, monitored by emission spectroscopy; conditions: [Ru] = 5 µM, P/D = 100, [NaCl] = 150 mM, TrisHCl = 10 mM (pH 7).

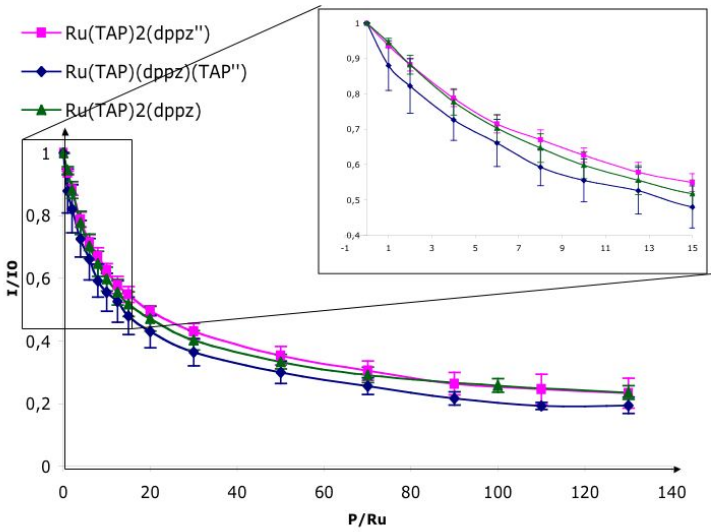

Figure S6. Affinity study of the free **$[Ru(TAP)_2(dppz)]^{2+}$** complex and derivatives **Ru(D)** and **Ru(T)**, with CT-DNA: titration of CT-DNA with the complexes monitored by emission spectroscopy; [Ru] = 5 µM; TrisHCl = 10 mM (pH 7), [NaCl] = 150 mM.

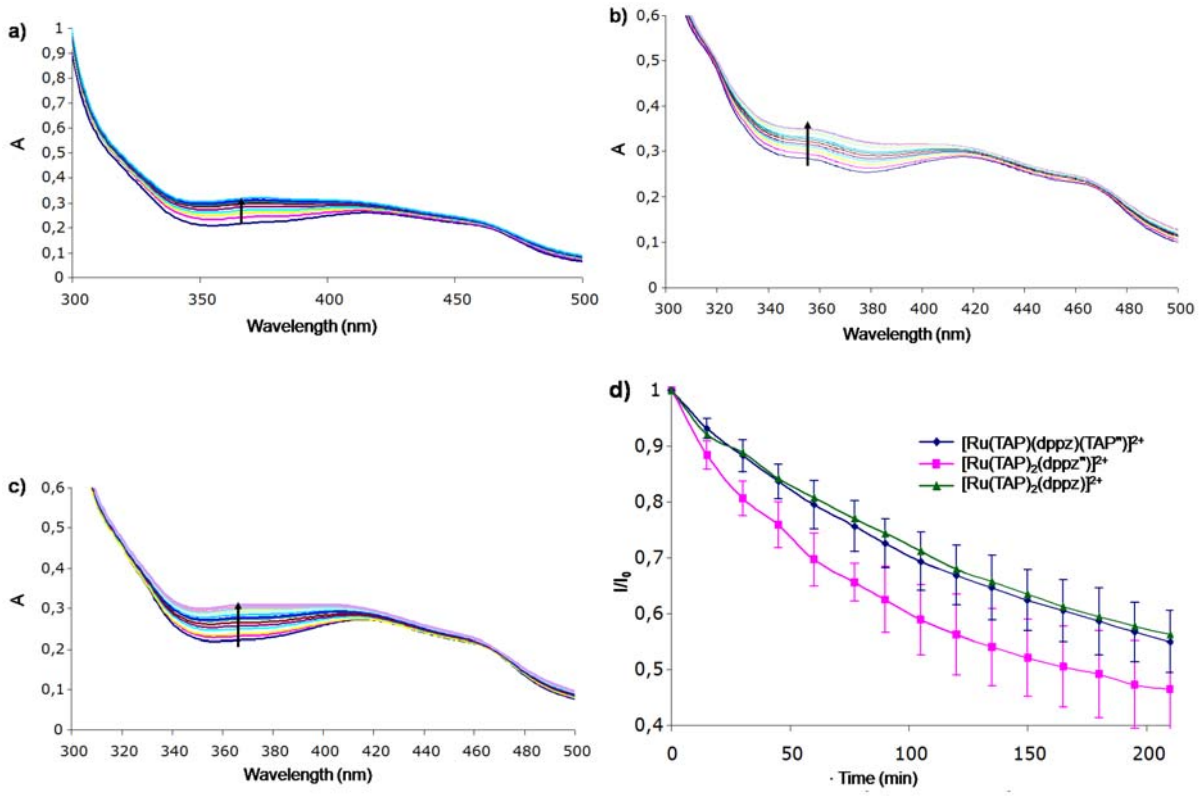

Figure S7. Evolution of the absorption spectra of the free **[Ru(TAP)$_2$(dppz)]$^{2+}$** complex and derivatives in presence of CT-DNA with the illumination time (up to 200 min): (a) **[Ru(TAP)$_2$(dppz")]$^{2+}$** (**Ru(D)**), (b) **[Ru(TAP)(dppz)(TAP")]$^{2+}$** (**Ru(T)**), (c) **[Ru(TAP)$_2$(dppz)]$^{2+}$**. Evolution of the emission intensity at λ_{max} for the free **[Ru(TAP)$_2$(dppz)]$^{2+}$** complex and derivatives in presence of CT-DNA, with the illumination time (d); conditions: [Ru] = 10 µM, [CT-DNA] = 10^{-3} M, [NaCl] = 150 mM, TrisHCl = 10 mM (pH 7).

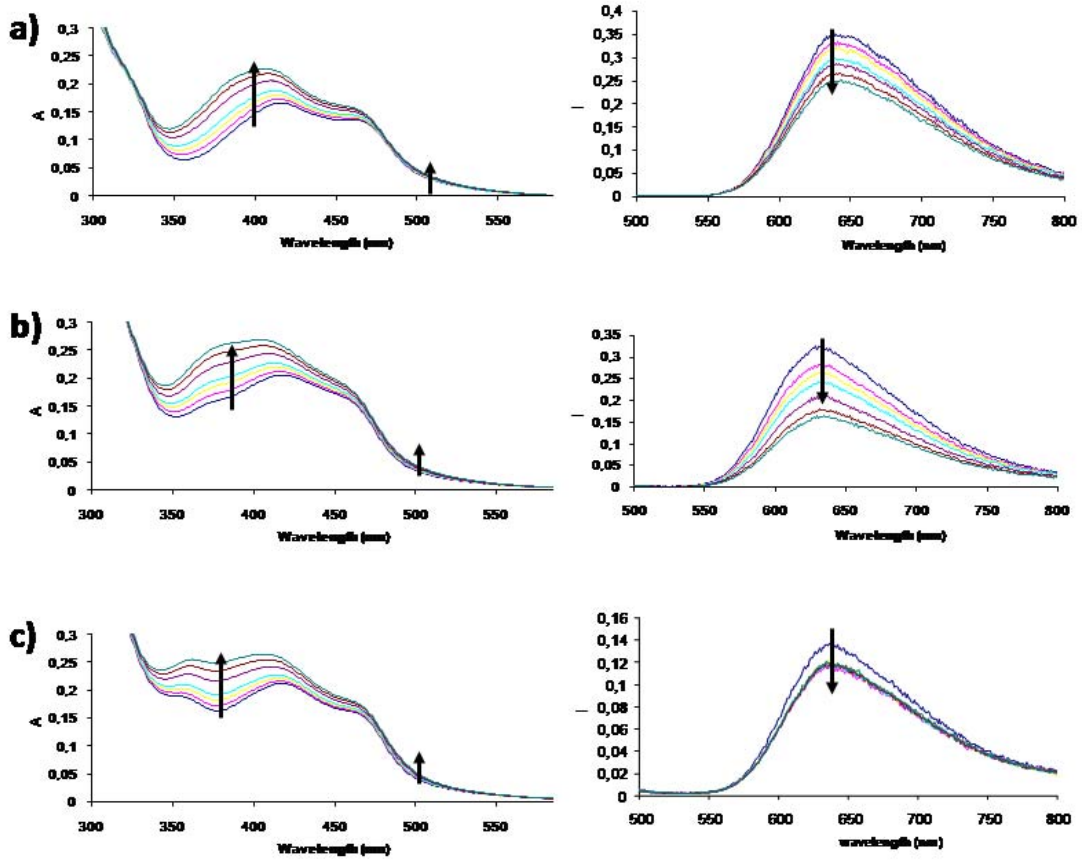

Figure S8. Evolution of the absorption (left) and emission (right) spectra of the Ru-ODN conjugates with illumination time (up to 60 min): (a) **Ru(P)-ODN$_{(G)}$**, (b) **Ru(D)-ODN$_{(G)}$** and (c) **Ru(T)-ODN$_{(G)}$**; conditions: Xe 500 W lamp, [Ru] = 10 μM, TrisHCl = 10 mM (pH 7), NaCl = 150 mM.